Journal of Applied Physics

Diffusion of boron in germanium at 800–900 °C revisited

Felix Kipke (iD), Tobias Südkamp, Jan K. Prüßing (iD), Dominique Bougeard, and Hartmut Bracht (iD)

COLLECTIONS

Paper published as part of the special topic on Defects in Semiconductors 2020
Note: This paper is part of the Special Topic on Defects in Semiconductors 2020.

View Online   Export Citation   CrossMark

ARTICLES YOU MAY BE INTERESTED IN

Reduction of threading dislocation density in top-down fabricated GaN nanocolumns via their lateral overgrowth by MOCVD
Journal of Applied Physics **127**, 025306 (2020); https://doi.org/10.1063/1.5110602

Effects of annealing on photoluminescence and defect interplay in ZnO bombarded by heavy ions: Crucial role of the ion dose
Journal of Applied Physics **127**, 025701 (2020); https://doi.org/10.1063/1.5134011

Electronic states and interband tunneling conditions in type-II quantum well heterostructures
Journal of Applied Physics **127**, 025705 (2020); https://doi.org/10.1063/1.5133801

Diffusion of boron in germanium at 800–900 °C revisited

Felix Kipke,[1,a)] (ID) Tobias Südkamp,[1] Jan K. Prüßing,[1] (ID) Dominique Bougeard,[2] and Hartmut Bracht[1,b)] (ID)

AFFILIATIONS

[1]Institute of Materials Physics, University of Münster, Wilhelm-Klemm-Straße 10, 48149 Münster, Germany
[2]Institut für Experimentelle und Angewandte Physik, Universität Regensburg, 93040 Regensburg, Germany

Note: This paper is part of the Special Topic on Defects in Semiconductors 2020.
a)**Electronic mail:** f.kipke@uni-muenster.de
b)**Electronic mail:** bracht@uni-muenster.de

ABSTRACT

Diffusion of boron (B) in germanium (Ge) at temperatures ranging between 800 °C and 900 °C is revisited following the most recent results reported by Uppal *et al.* [J. Appl. Phys. **96**, 1376 (2004)] that have been obtained mainly with implantation doped samples. In this work, we determined the intrinsic B diffusivity by employing epitaxially grown alternating undoped and B-doped Ge layer structures with three different dopant concentrations of 4×10^{17} cm^{-3}, 1×10^{18} cm^{-3}, and 3×10^{18} cm^{-3}. The diffusional broadening of B was analyzed by means of secondary ion mass spectrometry (SIMS) and numerically described to determine the diffusion coefficient. Additional SIMS analyses revealed a gradient in the oxygen (O) background concentration of the epitaxially doped Ge structure. A high O content observed in near-surface regions correlates with enhanced B diffusion. In contrast, B-doped regions with low O content showed a significantly lower B diffusivity representing the intrinsic diffusivity. The B diffusion coefficients are significantly lower compared to literature data and best described by a diffusion activation enthalpy and a pre-exponential factor of (4.09 ± 0.21) eV and 265^{+2256}_{-237} cm^2 s^{-1}, respectively.

I. INTRODUCTION

Over the past decade, germanium (Ge) as material for electronic applications has received some attention due to its promising application in silicon (Si) based integrated circuit technology.[1–3] Using Ge or SiGe epitaxial layers instead of Si, one can take advantage of the higher carrier mobility in Ge-rich layers.[4] Since doping of semiconductors is essential for the fabrication of electronic devices, the properties of n-type dopants, such as phosphorus (P),[5–14] arsenic (As),[6,8,9,13,15–17] and antimony (Sb),[6,8,9,18] and p-type dopants, such as boron (B),[12,19–23] aluminum (Al),[24] gallium (Ga),[25,26] and indium (In)[27] in Ge, have been the subject of numerous studies. In particular, the diffusion of these dopants in Ge under intrinsic[8,19,24,26,27] and extrinsic[8,10,14–17,27] doping conditions as well as under thermal equilibrium[8,19,24,26,27] and nonequilibrium[12,20,22,23] conditions has been investigated in order to characterize the atomic mechanisms of diffusion and the type of point defects involved. Based on these diffusion studies, the vacancy mechanism with doubly negatively charged vacancies V^{-2}

and singly negatively charged dopant-vacancy pairs XV^-,[8,9,17]

$$XV^- \rightleftharpoons X_s^+ + V^{2-}, \tag{1}$$
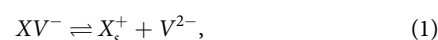
has been identified as the dominant mechanism that mediates the diffusion of mainly substitutionally dissolved n-type dopants X_s with $X \in \{P, As, Sb\}$.[8] Moreover, the mechanism that causes deactivation of n-type dopants in Ge during diffusion could be identified as a defect reaction,

$$XV^- + X_s^+ \rightleftharpoons X_2V^0, \tag{2}$$
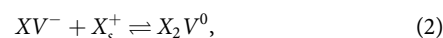
between the mobile singly negatively charged dopant-vacancy pair XV^- and the virtually immobile singly positively charged substitutional donor atom X_s^+.[9] This reaction forms neutral X_2V^0 dopant-vacancy complexes that upon cooling to room temperature can serve as the nucleation site for the formation of other stable defect clusters whose concentrations and specific structures will depend

on cooling.[28] Various dopant-defect clusters have been predicted by theoretical calculations[28] to contribute to donor deactivation and some of which have been verified by positron annihilation spectroscopy.[29,30]

Compared to the present understanding of the atomic mechanisms mediating the diffusion and deactivation of n-type dopants in Ge,[8,9,28,31,32] our knowledge on p-type dopants is less comprehensive. Considering the diffusion behavior of In and Ga in Ge neither a dopant deactivation nor a strongly enhanced diffusion under extrinsic doping is observed.[26,27] This is consistently described on the basis of the vacancy mechanism[27,28]

$$XV^- \rightleftharpoons X_s^- + V^0 \qquad (3)$$

with mobile dopant-vacancy pairs XV^- that are singly negatively charged, i.e., dopant-vacancy pairs possess the same charge state as the substitutional acceptors X_s^-. The vacancy involved in the diffusion mechanism (3) is mainly in its neutral charge state under p-type doping as determined by the impact of doping on self-diffusion in Ge.[33] The similarity in the diffusion behavior of Al, Ga, and In, which is close to Ge self-diffusion in magnitude, suggests that the vacancy mechanism (3) mainly mediates the diffusion of these p-type dopants X with $X \in \{Al, Ga, In\}$.[27,28]

In contrast, the diffusion of B in Ge is several orders of magnitude lower compared to Al, Ga, and In and described by a diffusion activation enthalpy of (4.65 ± 0.3) eV[19] that exceeds the corresponding values of Al $(3.45\,eV)$,[24] Ga $(3.21\,eV)$,[26] In $(3.51\,eV)$,[27] and Ge $(3.13\,eV)$[34] by more than 1 eV. The high activation enthalpy of B diffusion in Ge is assumed to indicate that self-interstitials mediate the diffusion process.[19] In fact, a dominance of self-interstitials in B diffusion has been verified by studies under nonequilibrium conditions, that is, by experiments that maintain a supersaturation of self-interstitials during diffusion.[12,20,22,23] Moreover, theoretical calculations confirm a self-interstitial rather than vacancy mediated diffusion of B in Ge.[35,36] Accordingly, general agreement on the mechanism of B diffusion in Ge seems to exist.[37]

The most recent and trustworthy study on B diffusion in Ge was performed by Uppal et al.[19] The authors mainly utilized B-implanted Ge samples for their diffusion experiments performed at temperatures between 800 °C and 900 °C. A single result reported for B diffusion in an epitaxially grown B-doped Ge structure is lower than data deduced from implantation doped samples. Uppal et al. argue that the deviation in the B diffusion coefficients of implanted and epitaxially grown material lies within the experimental errors.

The apparent lower B diffusion coefficient in epitaxially doped Ge and the limited temperature range considered by Uppal et al.[19] for their diffusion study motivated us to perform experiments with epitaxially B-doped Ge structures. Moreover, we tried to extend the diffusion experiments to lower temperatures to obtain a wider temperature range for a more accurate determination of the diffusion activation enthalpy. We obtained significantly lower values for B diffusion in epitaxially doped structures compared to the data reported by Uppal et al. for implantation doped samples. In accord with the former work, only B diffusion data for temperatures between 800 °C and 900 °C could be determined. Experiments below 800 °C failed due to severe Ge surface degradation that has hindered an accurate analysis of the B diffusion profiles by means

of secondary ion mass spectrometry (SIMS). The unexpected challenge to study B diffusion for temperatures below 800 °C is discussed and explained by Ge corrosion, that becomes significant, in particular, for the long annealing times at low temperatures.

II. EXPERIMENTAL

For studying B diffusion in Ge, an approximately 700 nm thick epitaxial Ge layer structure with alternating undoped and B-doped regions was grown by means of molecular beam epitaxy (MBE) on top of a (100)-oriented high ohmic (30 Ω cm) p-type single crystalline Ge wafer. The structure consists of three B-doped layers each about 100 nm in thickness and separated among by 100 nm thick undoped Ge. Dopant concentrations of about 4×10^{17} cm^{-3}, 1×10^{18} cm^{-3}, and 3×10^{18} cm^{-3} were established by MBE that are below the intrinsic carrier concentration $n_i(900°) = 9.4 \times 10^{18}$ cm^{-3} and $n_i(800°C) = 6.3 \times 10^{18}$ cm^{-3} of the diffusion temperature range.[8] Accordingly, our study of B diffusion performed by means of epitaxially doped Ge structures reflects the diffusion behavior under electronically intrinsic conditions.

Samples with lateral dimensions of approximately (2×2) mm^2 were cut from the wafer and cleaned with acetone and methanol. Subsequently, the samples were placed in high purity quartz ampoules, flushed with argon, evacuated to 10^{-5} mbar, and finally sealed. Diffusion annealing was performed at temperatures between 800 °C and 900 °C. After the thermal treatments, topography analysis was performed by means of non-contact atomic force microscopy (AFM). A mean roughness of $\lesssim 2$ nm was determined. Compared to the diffusional broadening of the B profiles in the range of $2\sqrt{Dt} = 19$ nm to $2\sqrt{Dt} = 25$ nm, the surface roughness does not affect the measurement of the B profiles significantly. The distribution of B was measured with time-of-flight SIMS (ToF-SIMS) utilizing 1 keV oxygen ions for sputtering and 25 keV bismuth cluster ions (Bi$_3$) for analysis. The BO_2^- signal is used to characterize the B profile (negative ion mode). Additional ToF-SIMS measurements were conducted to determine the O-concentration profiles of selected samples. The oxygen signal is measured in the negative ion mode (O$^-$) by sputtering with 2 keV cesium (Cs) ions. The analysis was performed with 25 keV Bi ions. B- and O-implanted calibration samples were used to convert the measured signals to the corresponding chemical concentrations. In order to achieve high sensitivity for the detection of B and O with ToF-SIMS, the concentration profiles of these elements were measured separately, that is, on different positions on the sample.

III. RESULTS

Figures 1 and 2 show B diffusion profiles measured with ToF-SIMS after annealing at 875 °C and 850 °C for 60 and 180 min, respectively. Compared to the as-grown structure, a pronounced broadening is observed. In order to extract the B diffusion coefficient D_B from the experimental profiles, Fick's second law of diffusion,

$$\frac{\partial C_B(x, t)}{\partial t} = D_B \frac{\partial^2 C_B(x, t)}{\partial x^2}, \qquad (4)$$
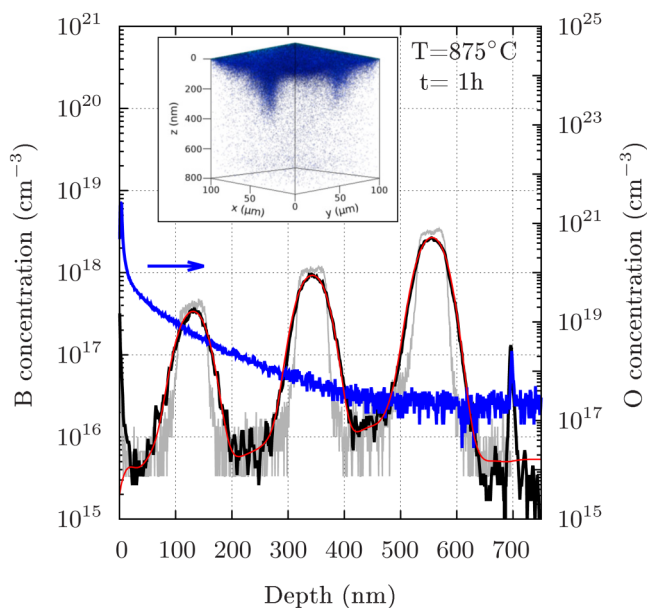
FIG. 1. ToF-SIMS concentration depth profiles of boron (B) (black) and oxygen (O) (blue) after annealing at 875 °C for 60 min in comparison to the as-grown B-doped Ge epitaxial layer structure (gray). After annealing, a diffusional broadening of the B profile was measured with ToF-SIMS. The O profile reveals a high concentration at the surface that decreases with increasing depth to the ToF-SIMS detection limit. The O profile is caused by an inhomogeneous O distribution. This is evidenced by the inset that shows the O distribution within a 3D measurement volume with a dimension of $100\,\mu m \times 100\,\mu m \times 800\,nm$. The intensity indicates the O content, the darker the spot, the higher the oxygen content. The homogeneous broadening of the three B-doped regions is described by a single effective diffusion coefficient of $3.1 \times 10^{-16}\,cm^2\,s^{-1}$. This demonstrates that B diffusion is not significantly affected by O for concentrations close to and below $10^{19}\,cm^{-3}$ in a measurement volume.
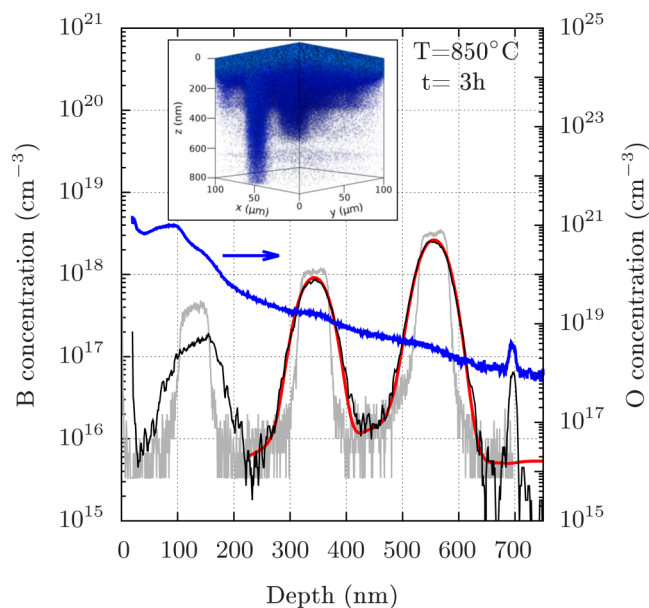

FIG. 2. ToF-SIMS concentration depth profiles of B (black) and O (blue) after annealing at 850 °C for 3 h. The B distribution of the as-grown layer structure (gray) is shown for comparison. The O profile within the region of the first B-doped Ge layer reveals an O concentration clearly above $10^{19}\,cm^{-3}$. The corresponding 3D distribution of O obtained for the measurement volume of $100\,\mu m \times 100\,\mu m \times 800\,nm$ is illustrated by the inset. The diffusional broadening of the near-surface B peak appears disturbed and stronger compared to the broadening of the deeper B peaks. This enhanced B diffusion is considered to be affected by oxygen. The broadening of the second and third B peaks is accurately described by a single effective diffusion coefficient of $1.1 \times 10^{-16}\,cm^2\,s^{-1}$. Obviously, the mean O concentration close to and below $10^{19}\,cm^{-3}$ in the range of this measurement volume does not significantly affect B diffusion.

was solved numerically. The as-grown B profile was considered as initial B distribution. Equation (4) assumes a concentration-independent B diffusion coefficient. The high quality of the fits to the measured profiles justifies these assumptions. Best fits are shown in Figs. 1 and 2 by the red solid lines. The diffusional broadening of the three B-doped regions obtained after annealing at 875 °C for 60 min is accurately described by a single value of D_B, which indicates a homogeneous broadening across the entire layer structure (see Fig. 1). In contrast, analysis of the B distribution measured after annealing at 850 °C for 180 min reveals that only the diffusional broadening of the second and third B peaks located in the range of 300–400 nm and 500–600 nm, respectively, is accurately described by a single value of D_B (see Fig. 2). The first B peak close to the surface shows a stronger diffusional broadening. Such an enhanced diffusion of B in the region of up to 200 nm below the surface was also detected on samples annealed at temperatures below 850 °C. With decreasing temperature and increasing diffusion time, the anomalous broadening tends to reach the second B peak and finally the whole epitaxial layer.

Motivated by a study on Ge corrosion published by Smith *et al.*,[38] we analyzed the oxygen (O) distribution in both untreated

and annealed Ge. For this purpose, Cs instead of O was used as a sputter ion during ToF-SIMS profiling. Figure 3 shows O-concentration depth profiles and three-dimensional (3D) representations of the O distribution at two different positions of a polished Ge wafer without epitaxial layer before any heat treatment. The inset of Fig. 3 displays the 3D distribution of O obtained for a surface area of $100 \times 100\,\mu m^2$ up to a depth of 300 nm (left part) and 400 nm (right part). The number density of the dots reflects the level of oxygen detected at the surface (see the top part of the insets) and inside the sample. The local high oxygen concentration that extends in columns to a depth of 60 nm (left part of inset) and 400 nm (right part of inset) into the sample is characteristic for a corrosion attack of the Ge surface that likely has occurred in the laboratory environment.[39] The one-dimensional O profiles are displayed by solid lines in the corresponding color code. The O-containing region shown in the left inset gives rise to a 1D O profile that drops to the detection limit at a depth of about 60 nm. On the other hand, the 3D O distribution illustrated in the right inset suggests an O profile that extends much deeper into the material. The two 1D oxygen profiles look very much different although in both cases the profiles result from oxygen columns inside the Ge
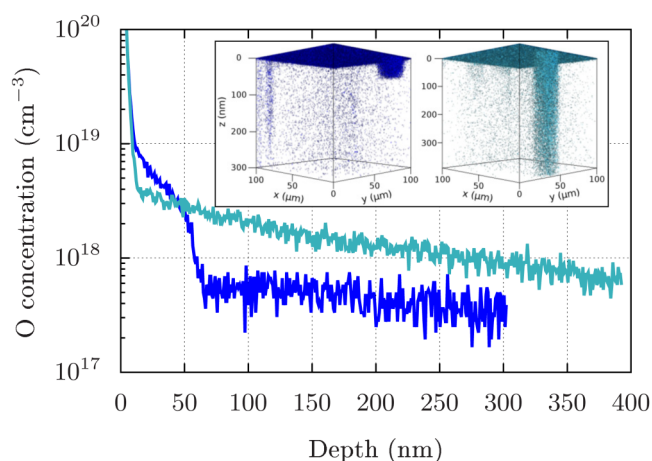
FIG. 3. One- and three-dimensional representation of the distribution of oxygen (O) measured with ToF-SIMS at two different positions of an untreated Ge wafer. The three-dimensional (3D) distribution of O is shown by the inserted figure in the same color code as the one-dimensional oxygen concentration depth profile deduced from the respective measurement volume.

FIG. 4. Concentration profile of the third boron peak of the Ge layer structure measured with ToF-SIMS after annealing at 850 °C for 3 h (black solid line). The B distribution of the as-grown layer structure is shown for comparison (gray solid line). The red line represents the numerical solution of Eq. (4) that best describes the experimental profile. The value determined for D_B is listed in Table I.

wafer. This demonstrates that 1D representations of oxygen profiles in Ge may not suggest the true distribution of this element.

The insets of Figs. 1 and 2 show 3D ToF-SIMS analyses of the lateral O distribution of the Ge samples annealed at 875 °C and 850 °C, respectively. The analyzed volumes span a surface area of $100 \times 100 \, \mu m^2$ and a depth of about 800 nm. A high O concentration is detected close to the surface (see the top part of the insets) that likely results from oxygen residues in the ampoule during annealing. In addition, an inhomogeneous spread of O into the Ge layer structure is detected, which is evident in the selective penetration of O into Ge that forms O-rich columns inside the Ge material. Apparently, the range of the Ge crystal affected by oxygen seems to be stronger correlated with the annealing time rather than with the temperature, i.e., the longer the time of annealing, the more pronounced the range of Ge affected by oxygen. Presumably, Ge surface corrosion proceeds during closed ampoule annealing due to oxygen or hydrogen-oxygen residues that could stem from the quartz ampoule, from the surface of the Ge samples, and/or from already corroded areas of Ge. Since B and O profiles can only be measured with different sputter ions, it is not possible to determine simultaneously the B and corresponding O profiles on the same sample area. SIMS analyses of the O distribution mainly reveal a high O concentration within the first 200 nm from the sample surface (see O profile of Figs. 1 and 2), whereas, at depths close to and above 500 nm, the O content detected with SIMS is below $10^{19} \, cm^{-3}$ or approaches the detection limit of 3–$4 \times 10^{17} \, cm^{-3}$. Accordingly, the diffusion coefficient determined from the diffusional broadening of the third B peak is assumed not to be affected by oxygen. Figure 4 shows the third peak of the B-doped Ge layer structure after annealing at 850 °C for 3 h. The experimental B diffusion profile is accurately described by a single concentration-independent B diffusion coefficient. The data deduced from the numerical simulation of the diffusional
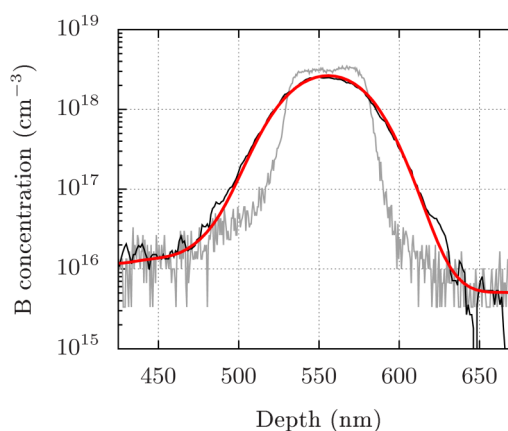
broadening of the third B peak from all samples annealed at temperatures between 805 °C and 900 °C are illustrated in Fig. 5 compared to the results reported by Uppal et al.[19] Our work reveals lower values for B diffusion in Ge than that of Uppal et al. The red solid line in Fig. 5 displays the temperature dependence of B diffusion, which is described by

$$D_B = 265^{+2256}_{-237} \exp\left(-\frac{(4.09 \pm 0.21)\,eV}{k_B T}\right) cm^2 \, s^{-1} \qquad (5)$$

and obtained by fitting an Arrhenius expression to the experimental data summarized in Table I. The temperature dependence of the diffusion coefficients of the p-type dopants Al,[24] Ga,[26] and In[27] as well as that of Ge self-diffusion[34] is displayed for comparison.

IV. DISCUSSION

Figure 5 reveals that our data on B diffusion in Ge are significantly lower than those of Uppal et al.[19] Uppal et al. mainly utilized B-implanted Ge samples for their diffusion experiments. They also prepared an epitaxial B-doped Ge layer and analyzed the broadening of the B profile after annealing at 875 °C for 12 h. A lower value of D_B was obtained (see the gray solid square in Fig. 5) but it was argued that this value is consistent with the data deduced from the ion-implanted samples. Whether the disparity in the former D_B data of implantation and epitaxial B-doped Ge is significant remains unsolved. Likewise, an impact of oxygen on B diffusion can hardly be verified because O profiles were not reported by Uppal et al.[19] However, since Uppal also preferred closed ampoule annealing and their B profiles are in a region of 200 nm below the surface, an impact of oxygen cannot be excluded.

After annealing, our epitaxial B-doped multilayers reveal B diffusivities in the range of the first B peak that are approximately a
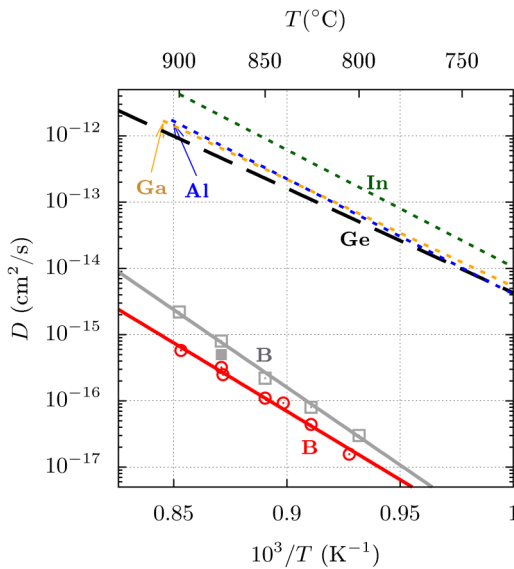
FIG. 5. Temperature dependence of the B diffusion coefficient in Ge determined in this work (red circles and red solid line) in comparison to the results reported by Uppal et al.[19] (gray symbols and gray solid line). The gray open and solid squares represent data obtained from Ge samples doped with B by ion implantation and *in situ* during epitaxial growth, respectively. The red (gray) solid line shows the temperature dependence of B diffusion that is best described by an activation enthalpy of $Q = (4.09 \pm 0.21)$ eV [(4.65 $\pm$ 0.3) eV] and a pre-exponential factor of $D_0 = 265^{+2256}_{-237}$ cm^2 s^{-1} ($D_0 = 1.97 \times 10^5$ cm^2 s^{-1}). The reported diffusion temperature dependence of the p-type dopants Al,[24] Ga,[26] In,[27] and Ge self-diffusion[34] is shown for comparison.

TABLE I. Diffusion coefficients D_B of boron in germanium determined from the boron-doped epitaxial layer structure after annealing at the temperatures T and times t indicated. The data represent the diffusional broadening of the third boron-doped layer that is located in the range of 500–600 nm beneath the surface. This region of the Ge layer structure is not significantly affected by oxygen that penetrates into the layer during diffusion annealing.

T (°C)	t (min)	D_B (cm^2 s^{-1})
805	1440	1.6×10^{-17}
825	600	4.4×10^{-17}
840	180	9.3×10^{-17}
850	180	1.1×10^{-16}
874	60	2.5×10^{-16}
875	60	3.1×10^{-16}
900	30	5.8×10^{-16}

factor of two higher than those describing the broadening of the third B peak. On the other hand, the broadening of the second and third B peaks is either very similar or deviates by not more than 20%. Thereby, mainly the second peak broadens stronger than the third one. This systematic led us to conclude that the data determined from the diffusional broadening of the third peak represent a good measure for B diffusion in Ge under electronically intrinsic and thermal equilibrium conditions.

The B diffusion activation enthalpy of $Q = 4.09$ eV[19] exceeds the activation enthalpy $Q = 3.13$ eV[34] of self-diffusion by about 1 eV. Evaluating the diffusion of B in Ge under intrinsic and local equilibrium conditions on the basis of the vacancy $XV \rightleftharpoons X_s + V$ and interstitialcy $XI \rightleftharpoons X_s + I$ mechanisms,[40] with I representing the Ge interstitial, the diffusion coefficient D_B equals either[41]

$$D_B = \frac{C_{BV}^{eq} D_{BV}}{C_{B_s}^{eq}} \quad \text{or} \quad D_B = \frac{C_{BI}^{eq} D_{BI}}{C_{B_s}^{eq}}. \quad (6)$$

In the framework of the vacancy mechanism that mainly mediates the diffusion of n-type dopants and other p-type dopants in Ge (see Sec. I), the higher activation enthalpy of B compared to self-atom diffusion points to a repulsive interaction between the dopant and the vacancy that is confirmed by theoretical calculations.[42,43] On the other hand, assuming the interstitialcy

mechanism, the high diffusion activation enthalpy of B diffusion suggests a high formation enthalpy of self-interstitials that has also been confirmed by theoretical studies.[35,36] In fact, the calculations of Janke et al.[36] yield an activation enthalpy of 4.3 eV for B diffusion in Ge via self-interstitials, which is in good agreement with our result considering the accuracy of the theoretical and experimental work. Since the behavior of B diffusion in Ge under intrinsic and thermal equilibrium conditions can be explained on the basis of both the vacancy and the interstitialcy mechanism, it still remains unsolved which mechanism dominates B diffusion in Ge under electronically intrinsic and thermal equilibrium conditions. Experiments on B diffusion under nonequilibrium conditions, i.e., experiments that, e.g., create a supersaturation of self-interstitials compared to thermal equilibrium, reveal a strong enhancement of B diffusion in Ge.[12,20,22,23,37] The enhanced B diffusion supports a self-interstitial mediated diffusion under the nonequilibrium conditions realized by irradiation but does not provide direct evidence on the mechanism mediating B diffusion in thermal equilibrium.

The SIMS measurements performed in the framework of this work reveal various levels of O concentrations before and after annealing. Unfortunately, O and B cannot be recorded simultaneously with ToF-SIMS (see Sec. II). This hinders to detect direct correlations in the O and B profiles and thus to identify possible defect reactions among these foreign atoms. Certainly, regions with high O concentrations reveal higher B diffusivities than regions with low concentrations. Scapellato et al.[44] report an impact of O by the formation of GeO$_2$ nanoclusters on B diffusion in Ge. The structural transformation of the nanoclusters formed in O-implanted Ge upon annealing inject self-interstitials that is evidenced in an enhanced B diffusion. A formation and transformation of GeO$_2$ nanoclusters could have also affected the broadening of the B peaks in regions with high oxygen content. Cross-sectional transmission electron microscopy analyses will be performed to verify the presence of GeO$_2$ nanoclusters in our epitaxial B-doped multilayers. The results of these investigations will be published elsewhere.

The observed impact of O on B diffusion in Ge raises the question whether O and, in particular, an unintentional doping with O may have affected experimental studies on the diffusion of

n-type and other p-type dopants in Ge reported in the literature. This is highly unlikely since no irregularities have been observed in the diffusion behavior of, e.g., the n-type dopants phosphorous, arsenic, and antimony and the p-type dopant indium for temperatures between 600 °C and 900 °C.[8,27] The challenge to extend B diffusion experiments to temperatures below 800 °C is due to the long annealing time that is required to determine a diffusional broadening of B with SIMS that is significantly longer than for other dopants in Ge because the B diffusivity is several orders of magnitude lower (see Fig. 5). Accordingly, the risk to corrode the Ge surface during B diffusion for long times of annealing at temperatures below 800 °C is quite high. Additional studies on the diffusion behavior and reaction of oxygen in Ge could reveal more information as our understanding of the property of oxygen in Ge is presently still limited.[45]

V. CONCLUSION

We have studied the diffusion of boron in epitaxially doped germanium multilayer structures at temperatures between 800 °C and 900 °C and obtained significantly lower B diffusion coefficients than those reported in the literature for implantation doped samples. The temperature dependence of B diffusion is best described by a diffusion activation enthalpy and a pre-exponential factor of (4.09 ± 0.21) eV and 265^{+2256}_{-237} cm^2 s^{-1}, respectively. The results represent diffusion data for thermal equilibrium and electronically intrinsic conditions and form a benchmark to identify nonequilibrium and doping effects in the diffusion behavior of B in Ge under different experimental conditions. Experiments performed to extend the temperature dependence of B diffusion to lower temperatures failed due to severe surface degradation. Oxygen residues in the annealing environment that could stem from the quartz ampoule and/or already oxidized areas of the Ge sample are considered to be responsible for the surface degradation that seems to increase with increasing anneal time rather than temperature. This behavior points to a corrosion process that degrades the surface, in particular, during long time annealing. The diffusion of B is enhanced in regions with oxygen concentrations exceeding 10^{19} cm^{-3}, whereas for concentrations below 10^{19} cm^{-3} no significant impact on B diffusion is observed.

ACKNOWLEDGMENTS

REFERENCES

[1]C. Claeys and E. Simoen, *Germanium-based Technologies—From Materials to Devices* (Elsevier, Amsterdam, 2007).
[2]D. P. Brunco, B. De Jaeger, G. Eneman, J. Mitard, G. Hellings, A. Satta, V. Terzieva, L. Souriau, F. E. Leys, G. Pourtois, M. Houssa, G. Winderickx, E. Vrancken, S. Sioncke, K. Opsomer, G. Nicholas, M. Caymax, A. Stesmans, J. Van Steenbergen, P. W. Mertens, M. Meuris, and M. M. Heyns, J. Electrochem. Soc. **155**, H552 (2008).
[3]E. Simoen, J. Mitard, G. Hellings, G. Eneman, B. De Jaeger, L. Witters, B. Vincent, R. Loo, A. Delabie, S. Sioncke, M. Caymax, and C. Claeys, Mater. Sci. Semicond. Process. **15**, 588 (2012).
[4]S. M. Sze, *Physics of Semiconductor Devices* (Wiley, New York, 1981).
[5]S. Matsumoto and T. Niimi, J. Electrochem. Soc. **125**, 1307 (1978).
[6]C. O. Chui, K. Gopalakrishnan, P. B. Griffin, J. D. Plummer, and K. C. Saraswat, Appl. Phys. Lett. **83**, 3275 (2003).
[7]G. Luo, C.-C. Cheng, C.-Y. Huang, S.-L. Hsu, C.-H. Chien, W.-X. Ni, and C.-Y. Chang, Electr. Lett **41**, 1354 (2005).
[8]S. Brotzmann and H. Bracht, J. Appl. Phys. **103**, 033508 (2008).
[9]S. Brotzmann, H. Bracht, J. Lundsgaard Hansen, A. Nylandsted Larsen, E. Simoen, E. E. Haller, J. S. Christensen, and P. Werner, Phys. Rev. B **77**, 235207 (2008).
[10]Th. Canneaux, D. Mathiot, J. P. Ponpon, S. Roques, S. Schmitt, and Ch. Dubois, Mat. Sci. Eng. B **154–155**, 68 (2008).
[11]P. Tsouroutas, D. Tsoukalas, I. Zergioti, N. Cherkashin, and A. Claverie, J. Appl. Phys. **105**, 094910 (2009).
[12]H. Bracht, S. Schneider, J. N. Klug, C. Y. Liao, J. Lundsgaard Hansen, E. E. Haller, A. Nylandsted Larsen, D. Bougeard, M. Posselt, and C. Wündisch, Phys. Rev. Lett. **103**, 255501 (2009).
[13]P. Tsouroutas, D. Tsoukalas, and H. Bracht, J. Appl. Phys. **108**, 024903 (2010).
[14]Y. Cai, R. Camacho-Aguilera, J. T. Bessette, L. C. Kimerling, and J. Michel, J. Appl. Phys. **112**, 034509 (2012).
[15]E. Vainonen-Ahlgren, T. Ahlgren, J. Likonen, S. Lehto, J. Keinonen, W. Li, and J. Haapamaa, Appl. Phys. Lett. **77**, 690 (2000).
[16]H. Bracht and S. Brotzmann, Mater. Sci. Semicond. Process. **9**, 471 (2006).
[17]M. Naganawa, Y. Shimizu, M. Uematsu, K. M. Itoh, K. Sawano, Y. Shiraki, and E. E. Haller, Appl. Phys. Lett. **93**, 191905 (2008).
[18]G. N. Wills, Solid State Electron. **10**, 1 (1967).
[19]S. Uppal, A. F. W. Willoughby, J. M. Bonar, N. E. B. Cowern, T. Grasby, R. J. H. Morris, and M. G. Dowsett, J. Appl. Phys. **96**, 1376 (2004).
[20]E. Bruno, S. Mirabella, G. Scapellato, G. Impellizzeri, A. Terrasi, F. Priolo, E. Napolitani, D. De Salvador, M. Mastromatteo, and A. Carnera, Phys. Rev. B **80**, 033204 (2009).
[21]E. Napolitani, G. Bisognin, E. Bruno, M. Mastromatteo, G. G. Scapellato, S. Boninelli, D. De Salvador, S. Mirabella, C. Spinella, A. Carnera, and F. Priolo, Appl. Phys. Lett. **96**, 201906 (2010).
[22]G. G. Scapellato, E. Bruno, A. J. Smith, E. Napolitani, D. De Salvador, S. Mirabella, M. Mastromatteo, A. Carnera, R. Gwilliam, and F. Priolo, Nucl. Instrum. Methods Phys. Res. B **282**, 8 (2012).
[23]S. Schneider, H. Bracht, J. N. Klug, J. Lundsgaard Hansen, A. Nylandsted Larsen, D. Bougeard, and E. E. Haller, Phys. Rev. B **87**, 115202 (2013).
[24]P. Dorner, W. Gust, A. Lodding, H. Odelius, B. Predel, and U. Roll, Acta Metall. **30**, 941 (1982).
[25]U. Södervall, H. Odelius, A. Lodding, U. Roll, B. Predel, W. Gust, and P. Dorner, Philos. Mag. A **54**, 539 (1986).
[26]I. Riihimäki, A. Virtanen, S. Rinta-Anttila, P. Pusa, J. Räisänen, and The ISOLDE Collaboration, Appl. Phys. Lett. **91**, 091922 (2007).
[27]R. Kube, H. Bracht, A. Chroneos, M. Posselt, and B. Schmidt, J. Appl. Phys. **106**, 063534 (2009).
[28]A. Chroneos and H. Bracht, Appl. Phys. Rev. **1**, 011301 (2014).
[29]A. R. Peaker, V. P. Markevich, B. Hamilton, I. D. Hawkins, J. Slotte, K. Kuitunen, F. Tuomisto, A. Satta, E. Simoen, and N. V. Abrosimov, Thin Solid Films **517**, 152 (2008).
[30]J. Kujala, T. Südkamp, J. Slotte, I. Makkonen, F. Tuomisto, and H. Bracht, J. Phys. Condens. Matter **28**, 335801 (2016).
[31]H. Bracht, S. Schneider, and R. Kube, Microelectron. Eng. **88**, 452 (2011).
[32]J. Vanhellemont and E. Simoen, Mater. Sci. Semicond. Process. **15**, 642 (2012).
[33]T. Südkamp, H. Bracht, G. Impellizzeri, J. Lundsgaard Hansen, A. Nylandsted Larsen, and E. E. Haller, Appl. Phys. Lett. **102**, 242103 (2013).
[34]E. Hüger, U. Tietze, D. Lott, H. Bracht, D. Bougeard, E. E. Haller, and H. Schmidt, Appl. Phys. Lett. **93**, 162104 (2008).
[35]P. Delugas and V. Fiorentini, Phys. Rev. B **69**, 085203 (2004).
[36]C. Janke, R. Jones, S. Öberg, and P. R. Briddon, J. Mater. Sci. Mater. Electron. **18**, 775 (2007).

[37]S. Mirabella, D. De Salvador, E. Napolitani, E. Bruno, and F. Priolo, J. Appl. Phys. **113**, 031101 (2013).

[38]E. F. Smith, D. Briggs, and N. Fairley, Surf. Interface Anal. **38**, 69 (2006).

[39]T. Südkamp, "Characterization of atomic transport in nano-structured silicon and germanium to reveal properties of self- and foreign-atom defects," Doctoral dissertation (University of Münster, 2018).

[40]Under intrinsic diffusion conditions, the charge states of the individual point defects involved in the diffusion mechanisms do not affect the behavior of dopant diffusion and thus are not significant (see Ref. 41 for overview).

[41]H. Bracht, Phys. Rev. B **75**, 035210 (2007).

[42]A. Chroneos, B. P. Uberuaga, and R. W. Grimes, J. Appl. Phys. **102**, 083707 (2007).

[43]A. Chroneos, J. Appl. Phys. **107**, 076102 (2010).

[44]G. G. Scapellato, S. Boninelli, E. Napolitani, E. Bruno, A. J. Smith, S. Mirabella, M. Mastromatteo, D. De Salvador, R. Gwilliam, C. Spinella, A. Carnera, and F. Priolo, Phys. Rev. B **84**, 024104 (2011).

[45]E. N. Sgourou, Y. Panayiotatos, R. V. Vovk, N. Kuganathan, and A. Chroneos, Appl. Sci. **9**, 2454 (2019).